MOLECULAR AND CELLULAR BIOLOGY, Dec. 2001, p. 8398–8413 Vol. 21, No. 24
0270-7306/01/$04.00+0 DOI: 10.1128/MCB.21.24.8398–8413.2001

TIP49b, a Regulator of Activating Transcription Factor 2 Response to Stress and DNA Damage

SSANG-GOO CHO,[1] ANINDITA BHOUMIK,[1] LIMOR BRODAY,[1] VLADIMIR IVANOV,[1] BARRY ROSENSTEIN,[2] AND ZE'EV RONAI[1]*

The Ruttenberg Cancer Center[1] and Department of Radiology,[2] Mount Sinai School of Medicine, New York, New York 10029

Received 11 July 2001/Returned for modification 5 September 2001/Accepted 19 September 2001

Activating transcription factor 2 (ATF2/CRE-BP1) is implicated in transcriptional control of stress-responsive genes. A yeast two-hybrid screen identified TBP-interacting protein 49b (TIP49b), a component of the INO80 chromatin-remodeling complex, as a novel ATF2-interacting protein. TIP49b's association with ATF2 is phosphorylation dependent and requires amino acids 150 to 248 of ATF2 ($ATF2^{150–248}$), which are implicated in intramolecular inhibition of ATF2 transcriptional activities. Forced expression of TIP49b efficiently attenuated ATF2 transcriptional activities under normal growth conditions as well as after UV treatment, ionizing irradiation, or activation of p38 kinase, all of which induced ATF2 phosphorylation and increased TIP49b-ATF2 association. Constitutive expression of $ATF2^{150–248}$ peptide outcompeted TIP49b interaction with ATF2 and alleviated the suppression of ATF2 transcriptional activities. Expression of $ATF2^{150–248}$ in fibroblasts or melanoma but not in ATF2-null cells caused a profound G_2M arrest and increased degree of apoptosis following irradiation. The interaction between ATF2 and TIP49b constitutes a novel mechanism that serves to limit ATF2 transcriptional activities and highlights the central role of ATF2 in the control of the cell cycle and apoptosis in response to stress and DNA damage.

Activating transcription factor 2 (ATF2/CRE-BP1) is a member of the ATF-CREB family of transcription factors (28, 49), which have been implicated in growth control, cell cycle progression, differentiation, and transformation. As a leucine zipper transcription factor, ATF2 binds an 8-bp response element (CRE/URE; 5′-TGACGTCA-3′ [61]) as a homodimer or as a heterodimer with other members of the ATF family, as well as the Jun/Fos family of transcription factors (10, 17, 27, 69). Most common is the ATF2 c-Jun heterodimer, which recognizes the AP1/CRE target sequence (20, 69, 71). Upon its phosphorylation on Ser-121, ATF2 associates with p300/CBP, which links it to the basal transcriptional complex (39). Like p300, ATF2 was also reported to elicit histone acetyltransferase (HAT) activities that are increased upon its phosphorylation (38).

Several ATF2 isoforms (CRE-BP-1, -2, and -3), generated by differential splicing, elicit different transcriptional outputs (23). Full-length ATF2 (CRE-BP1) is transcriptionally inactive as a result of intramolecular interaction of its bZIP motif with the amino-terminal transactivation domain (43). Upon exposure to stress or DNA damage, JNK/p38 kinases phosphorylate T-69 and T-71, alleviating intrinsic inhibition and rendering ATF2 transcriptionally active (5, 18, 25, 47, 71). ATF2 can be also activated upon association with viral proteins, as shown for E1A (11, 21, 43, 46).

Although ATF2 has been implicated in the transcriptional control of various stress-responsive genes, including c-*jun* (71), beta interferon (19), transforming growth factor beta (41), and tumor necrosis factor alpha (TNF-α) (54, 68), our understanding of the biological functions of ATF2 is still limited. Several observations point to the role of ATF2 in the transformation process. ATF2 has been implicated in a transcriptional response mediated by the transforming adenovirus protein E1A (26, 45, 46, 69). Overexpression of ATF2 potentiates the ability of v-*jun*-transformed chicken embryo fibroblasts to grow in low-serum medium in vitro and to form tumors in vivo (30). The level of ATF2 mRNA is higher in human tumors than in normal tissues (67). Our studies revealed the contribution of ATF2 to the resistance of human melanoma cells to irradiation and chemical treatment, by altering the balance between TNF and Fas death signaling cascades (33, 60).

To further study mechanisms underlying ATF2's ability to modulate radiation resistance, the cell cycle, and apoptosis, we performed a yeast two-hybrid screen that led to the identification of TIP49b as a novel ATF2-interacting protein. TIP49b (35) (synonyms: TIP48 [73], Reptin52 [3], RUVBL2 [58], Rvb2 [65])], TAP54β [31], and TIH2p [24]) is a protein of 463 amino acids that exhibits 43% identity with TIP49a (36) (synonyms: Pontin52 [4])], NMP238 [29])], RUVBL1 [58], Rvb1 [65])], TAP54α [31], and TIH1p [40]).

TIP49b and TIP49a are expressed ubiquitously in all human tissues examined (50, 56). Both proteins are essential in yeast (35, 58), and *Drosophila* flies that are deficient in TIP49a and TIP49b die at an early developmental stage, indicating that both genes encode essential and nonredundant functions during early development (3).

TIP49a and TIP49b are members of a highly conserved protein family with homology to bacterial RuvB, an ATP-dependent DNA helicase that catalyzes branch migration in Holliday junctions. Mammalian TIP49a and TIP49b possess intrinsic ATPase activities that are stimulated by single-stranded DNA and helicase activities of opposite polarity (35, 51). Interaction of β-catenin with TIP49a/Pontin52 and

* Corresponding author. Mailing address: Ruttenberg Cancer Center, Mount Sinai School of Medicine, 1 Gustave Levy Place, Box 1130, New York, NY 10029. Phone: (212) 659-5571. Fax: (212) 849-2425. E-mail: zeev.ronai@mssm.edu.

TIP49b/Reptin52 (3, 4) results in altered TCF/LEF-mediated transcription. TIP49a/TIP49 and TIP49b/TIP48 have also been found in complex with c-Myc, which affects c-Myc-mediated oncogenic transformation (73). TIP49a/p50/Tih2p (40) and TIP49b/p47/Tih1p (24) have been implicated in cell cycle progression (44). The TIP49a/RUVBL1 gene maps to 3q21, a region with frequent rearrangements in both leukemias and solid tumors (37, 62).

The INO80 chromatin remodeling complex, which contains about 12 polypeptides, includes TIP49a/Rvb1 and TIP49b/Rvb2 (65). Like the related remodeling complexes SWI/SNF (15) and RSC (8), the INO80 complex exhibits DNA-dependent ATPase activity implicated in transcription as well as DNA damage repair (65). The findings of TIP49a and TIP49b/TIP48 in complex with c-Myc (73) and as part of the TIP60 HAT complex (31) further point to its role in diverse aspects of chromatin metabolism and transcriptional regulation of key cell cycle-regulatory proteins.

Here we report on the identification and characterization of a novel interaction between TIP49b and ATF2 which results in inhibition of ATF2 transcriptional activity and identifies the role that ATF2 plays in the control of cell cycle, DNA repair, and apoptosis.

MATERIALS AND METHODS

Cell culture and transfection. Human embryonic kidney (HEK) 293T cells, ATF2$^{-/-}$ (48), c-Jun$^{-/-}$ mouse fibroblasts (72), and mouse melanoma cells (K1735p) (55) were maintained in Dulbecco's modified Eagle's medium supplemented with 10% heat-inactivated fetal bovine serum and 100 U of penicillin and 100 U of streptomycin (Gibco-BRL) per ml in a 5% CO_2 incubator at 37°C (32). Normal fibroblasts and Myc$^{-/-}$ (HO15.19) (52) fibroblasts were grown in the presence of 10% calf serum. For DNA transfection, cells were plated in 100-mm dishes at a density of 2.5×10^6 cells/plate and transfected 18 h later with the respective expression vectors using the calcium phosphate method for 293T cells (12) or Lipofectamine-Plus for all other cell lines (Gibco-BRL).

DNA constructs. Hemagglutinin (HA)-tagged full-length ATF2 and the splice variant form of ATF2, ATF2Δ (Δ150–248), were constructed in the pEF-HA vector (a gift from Eugenia Spanopollou). The full-length TIP49b cDNA was amplified by PCR from a human melanoma cDNA library and cloned into pcDNA3 tagged with two Flags. TIP49b deletion mutants TIP49b-ΔC (amino acids [aa] 1 to 306) and TIP49b-CT (aa 307 to 463) were generated by PCR and cloned into pcDNA3-2Flag. Flag-tagged TIP49b-DN (D299N), which is designed to inactivate helicase activity, was constructed with the aid of the QuikChange site-directed mutagenesis kit (Stratagene). The DNA fragment corresponding to amino acids 150 to 248 of ATF2 was generated by PCR followed by in-frame cloning into pEF-HA (pEF-HA-Penetratin-ATF2$^{150–248}$-GFP) or a retroviral vector, pBabe (pBabe-ATF2$^{150–248}$-GFP). The integrity of all constructs was verified by sequencing. Flag-tagged TIP49a and TIP49a-DN (D302N) were a generous gift from M. D. Cole (73), and ΔN-ASK and MKK6-DD were kindly provided by H. Ichijo (63) and R. Davis, respectively.

Retroviral infection. Phoenix-eco or Phoenix-ampho packaging cells (generous gifts from G. P. Nolan) were infected using standard protocols (57).

Yeast two-hybrid screening. N-terminally truncated (Δ1–150) and full-length ATF2 cDNA fused to the *lexA* DNA-binding domain were used as bait to screen a human melanoma cDNA library for interacting proteins, using the protein trap yeast two-hybrid system. The bait was fused in frame with the LexA DNA-binding domain by subcloning into the *Bam*HI and *Not*I sites of PEG202. Preys were fused in frame with the B42 activation domain by subcloning into the *Eco*RI and *Xho*I sites of the P3G4-5 vector. A total of 8.5×10^6 yeast transformants were screened. cDNAs from positive colonies were rescued and subjected to PCR analysis. Clones that exhibited different restriction patterns were retested for specificity by transformation into yeast strains expressing the bait ATF2 protein.

Coimmunoprecipitation. 293T cells were cotransfected using the calcium phosphate method and lysed in F-buffer (10 mM Tris [pH 7.05]; 50 mM NaCl; 30 mM sodium pyrophosphate; 50 mM NaF; 5 μM $ZnCl_2$; 0.1 mM Na_3VO_4; 1% Triton X-100; 1 mM phenylmethylsulfonyl fluoride; 5 U of α_2-macroglobulin, 2.5 U of pepstatin, 2.5 U of leupeptin, and 2.8 μg of aprotinin per ml; and 150 μM benzamidine) (66).

Immunoprecipitations were carried out with anti-Flag antibody (Sigma) (4°C overnight) followed by incubation with protein G beads (Gibco-BRL). Bead-bound immune complexes were washed and subjected to sodium dodecyl sulfate-polyacrylamide gel electrophoresis (SDS-PAGE) followed by immunoblot analysis with antiphospho-(T69 and T71)-ATF2 (NEB), anti-ATF2 (Santa Cruz), or anti-HA antibodies (Babco) as indicated in Results. In all cases reactions were detected by means of enhanced chemiluminescence (Amersham). Interactions between endogenously expressed proteins were carried out using mouse monoclonal anti-ATF2 antibody (Santa Cruz) followed by immunoblot analysis with rabbit anti-TIP49b polyclonal antibody (a generous gift from T. Tamura).

Luciferase reporter assay and flow cytometric analysis. Cells were transiently transfected with reporter plasmids (0.02 μg) together with the expression vectors (0.2 to 0.4 μg) and pCMV-β-gal (0.03 μg). The reporter constructs used were 5xJun2-tk-Luc (70), −615 TNF-Luc or −615 TNF (mutCRE)-Luc (59) and TOPFLASH or FOPFLASH (42) luciferase reporter plasmids. The amount of DNA for each transfection was equalized by addition of the respective empty vectors. Luciferase activity was measured in a luminometer and normalized to the β-galactosidase activity in the same cells.

For cell cycle and apoptosis studies, cells were irradiated with UVC (60 J/m^2) or X-ray (5 Gy) and 6 to 48 h later were stained with propidium iodide followed by flow cytometric analysis using a FACSCalibur flow cytometer (Becton Dickinson, Mountain View, Calif.) and the CellQuest program.

RESULTS

Identification of TIP49b as an ATF2-associated protein. We employed the yeast two-hybrid system to identify ATF2-interacting proteins. Using full-length as well as amino-terminally truncated (Δ1–196) forms of ATF2 as bait, we screened 8×10^6 yeast colonies expressing a human melanoma cDNA library prepared 3 h after UV irradiation. Among the total of 270 positive colonies, we identified 23 different cDNAs, which were further confirmed for their association. Among the novel ATF2-associated proteins was the C-terminal domain of TIP49b (data not shown).

To confirm the interaction between ATF2 and TIP49b in mammalian cells, we coexpressed HA-ATF2 and Flag-TIP49b in HEK 293T cells. Immunoprecipitation of TIP49b followed by Western analysis confirmed the interaction between exogenously expressed ATF2 and TIP49b (Fig. 1A). Such association was not observed using an alternatively spliced form of ATF2 that lacks amino acids 150 to 248, suggesting that this region may be important for the interaction between ATF2 and TIP49b.

To demonstrate the association between endogenous ATF2 and exogenous TIP49b, cells were transfected with Flag-TIP49b and proteins were immunoprecipitated using antibodies to ATF2, followed by immunoblotting with antibodies to the Flag epitope (Fig. 1B). Further analysis was carried out on endogenous proteins via immunoprecipitation with antibodies to ATF2 and Western blotting with antibodies to TIP49b (Fig. 2a). All reactions revealed the association between TIP49b and ATF2.

TIP49b has homology with the bacterial RuvB proteins and contains Walker A and Walker B motifs, found in proteins that bind and hydrolyze ATP (73). A single missense mutation in the Walker B box (*D*EVH→ *N*EVH) is sufficient to abolish ATPase activities, as shown for RuvB (53). To determine whether mutation in the Walker B domain of TIP49b affects the interaction with ATF2, we generated Flag-TIP49b-DN (D299N) and tested its association with ATF2 (Fig. 1C). As

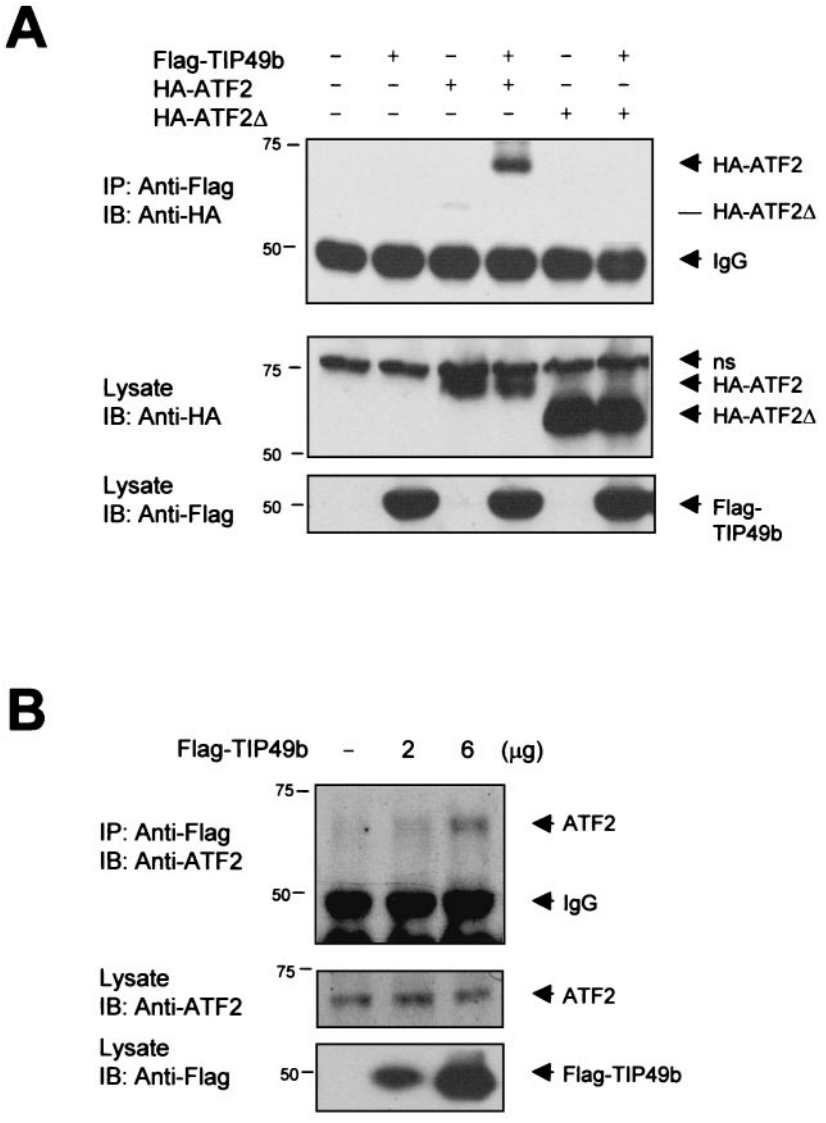

FIG. 1. TIP49b interacts with the full-length ATF2 but not with its ATF2Δ150–248 isoform. (A) HEK 293T cells were transiently transfected with HA-ATF2, HA-ATF2Δ (Δ150–248), and Flag-TIP49b as indicated. Lysates were immunoprecipitated (IP) using anti-Flag antibody and immunoblotted (IB) with anti-HA antibody. The two bottom panels verify expression of the respective proteins; ns, nonspecific band. In this and subsequent figures, sizes are shown on the left (in kilodaltons). (B) 293T cells were transiently transfected with Flag-TIP49b constructs (2 or 6 μg), and lysates were immunoprecipitated with anti-Flag antibody followed by immunoblotting (IB) with anti-ATF2 antibody (F2BR-1; anti-mouse immunoglobulin G [IgG]). In the lower panels, the levels of endogenous ATF2 and exogenously expressed Flag-TIP49b were analyzed by probing immunoblots with the indicated antibodies. (C) Schematic diagram of TIP49a, TIP49b, and their mutants. AAA (ATPases associated with various cellular activities) and DnaB (DnaB-like helicase) domains and the Walker motifs are indicated, with the mutation in the Walker B box used to make the TIP49DN mutants. (D) 293T cells were transiently transfected with indicted plasmids. Lysates were subjected to immunoprecipitation using anti-Flag antibody, and precipitated proteins were subjected to Western blot using anti-HA antibody. Lower panels depict direct Western blots to reveal expression of ATF2 and TIP49 forms. (E) 293T cells were transfected with Flag-TIP49b (WT), Flag-TIP49b-ΔC (aa 1 to 306), Flag-TIP49b-CT (aa 307 to 463) and HA-ATF2 as indicated. Lysates were immunoprecipitated with anti-Flag antibody and immunoblotted with anti-HA antibody. The expression of the exogenous proteins was verified in the lower panels.

shown in Fig. 1D, TIP49b-DN mutants interacted with ATF2 to the same extent as wild-type TIP49b.

We next assessed the ability of TIP49a and its mutant TIP49a-DN (D302N) to associate with ATF2. Neither TIP49a nor TIP49a-DN was found in complex with ATF2 (Fig. 1D). Lack of TIP49a association with ATF2, which is capable of association with TIP49b, provides the first example of selective association with one of the two TIP49 components.

To map the domains required for TIP49b association with ATF2, we generated two deletion mutants, one lacking the C-terminal domain (ΔC) and one that contains only the C-terminal region (CT) (Fig. 1C). Coimmunoprecipitation assays revealed interaction between the TIP49b-CT form and ATF2, albeit at a lower efficiency than with the wild-type protein. Such interaction was not seen with the TIP49b-ΔC form (Fig. 1E). This result is consistent with the initial yeast two-hybrid screen, where the cDNA encoding the C-terminal region (aa 307 to 463) of TIP49b was identified as an ATF2-interacting protein.

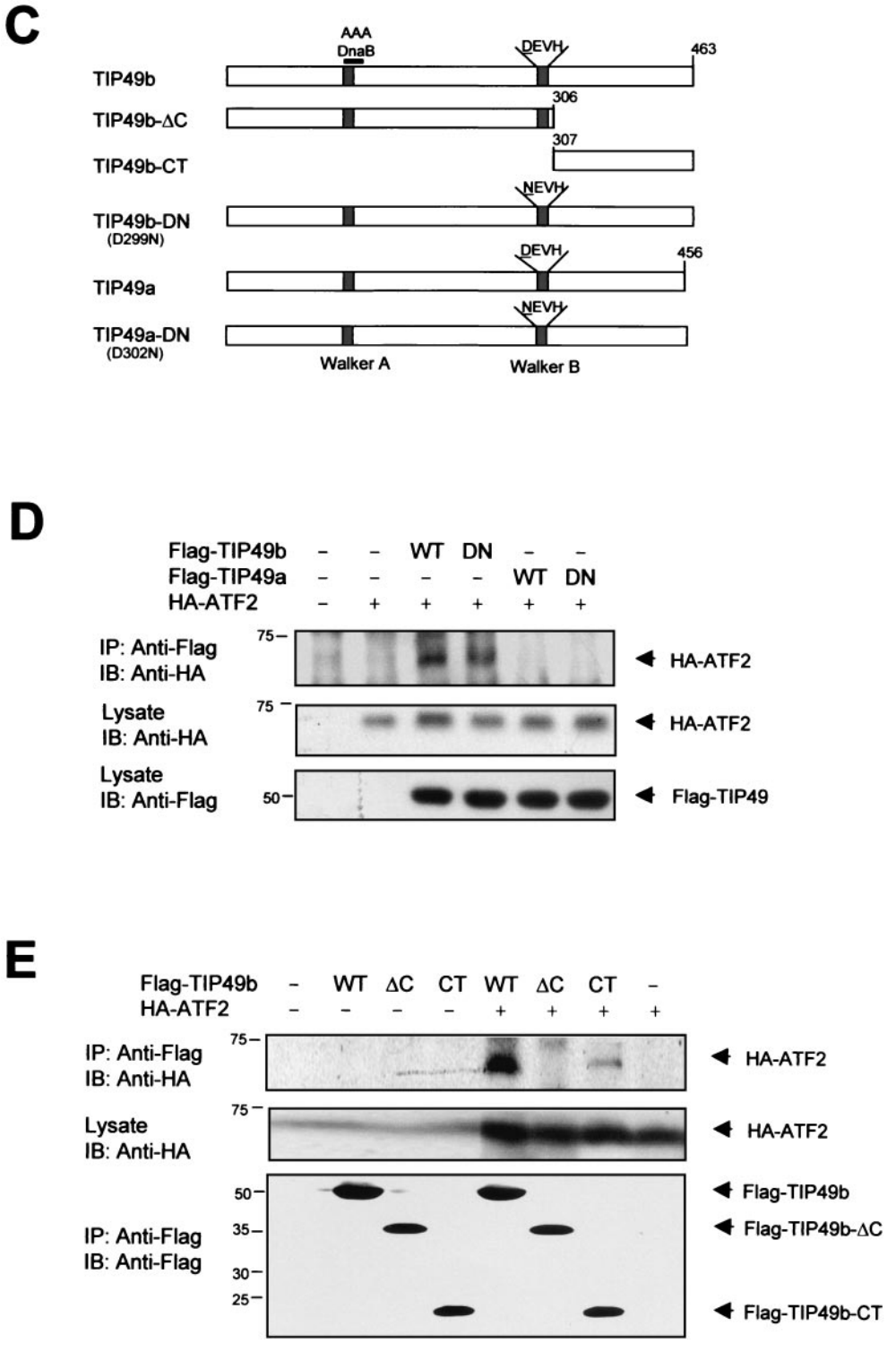

FIG. 1—*Continued.*

These findings suggest that the C-terminal domain of TIP49b is required for the association with ATF2.

Association of TIP49b with ATF2 coincides with ATF2 phosphorylation and is elevated in UV- and ionizing radiation (IR)-treated cells. Since TIP49b homologues have been implicated in DNA repair, we examined the effect of irradiation on the ATF2-TIP49b association. UV irradiation increased the association between endogenous ATF2 and TIP49b. Immunoprecipitation of TIP49b followed by analysis of bound ATF2 revealed a marked increase in the ATF2-TIP49b association within 1 h after UV treatment; this increase declined to basal levels as early as 2 h after irradiation. Elevated association of

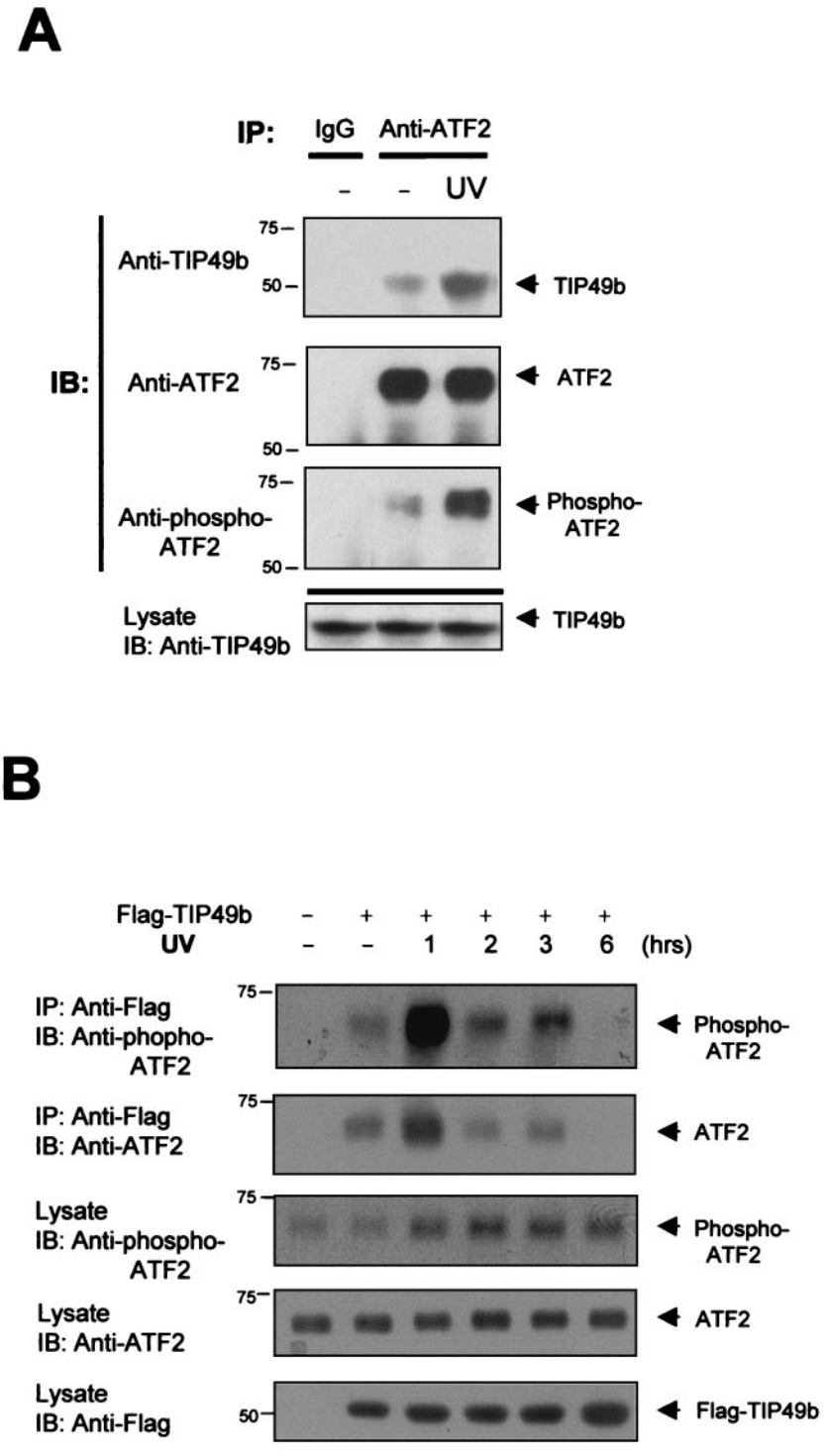

FIG. 2. Interaction between ATF2 and TIP49b is phosphorylation dependent. 293T cells were untreated or treated with UV (60 J/m^2), and protein extracts were prepared and subjected to immunoprecipitation (IP) with anti-ATF2 antibody (or with normal mouse preimmune IgG) followed by immunoblot (IB) with antibodies as indicted. (B and C) 293T cells were transfected with the Flag-TIP49b construct, and 24 h later cells were treated with UV (60 J/m^2) (B) or X-ray irradiated (X-ray; 5 Gy) (C). Protein extracts were prepared at indicated time points after treatment, immunoprecipitated, and immunoblotted with the indicated antibodies. (D) Cells were cotransfected with Flag-TIP49b and ΔN-ASK1 or MKK6-DD. Thirty-five hours after transfection, lysates were prepared and immunoprecipitated, followed by immunoblot with the indicated antibodies. (E) Cells were cotransfected with Flag-TIP49b and wild-type (WT) HA-ATF2 or mutant HA-ATF2 (T69A and T71A). To induce ATF2 phosphorylation, indicated cells were also cotransfected with MKK6-DD or treated with UV. After 6 h, lysates were prepared and immunoprecipitated using anti-Flag antibody. The immunoprecipitates were immunoblotted with anti-HA antibodies. The bottom panels verify expression of the exogenously expressed proteins.

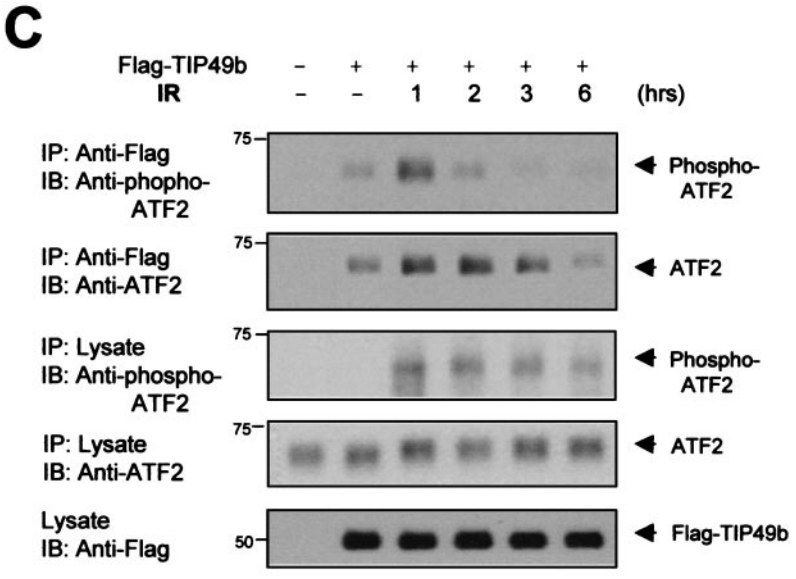

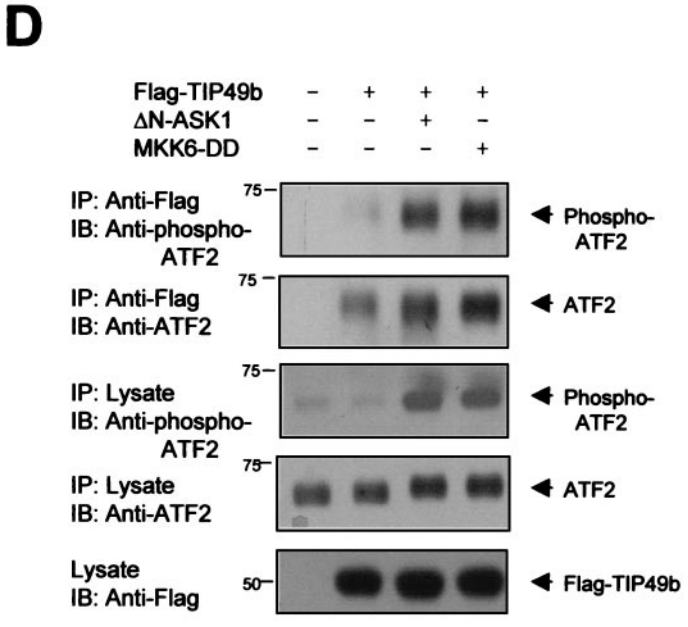

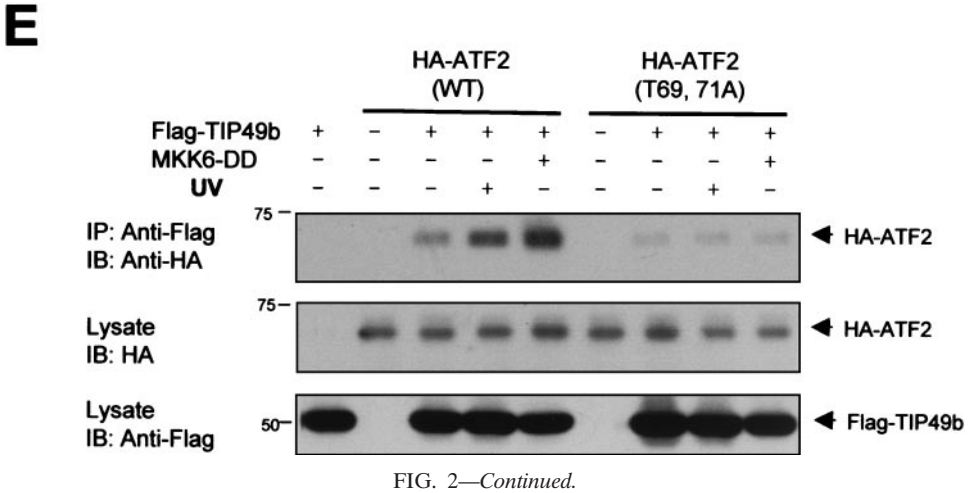

FIG. 2—*Continued.*

TIP49b and ATF2 coincided with a substantial increase in ATF2 phosphorylation on residues 69 and 71 (Fig. 2B).

These data suggest that the association of TIP49b with ATF2 is increased by UV treatment and that it may be phosphorylation dependent. Given that TIP49b is a homologue of RuvB, which is implicated in double-strand repair, we also elucidated the effect of IR on the association of TIP49b with ATF2. IR increased the interaction between ATF2 and TIP49b within 1 h after treatment and maintained the elevated association for longer time periods (up to 3 h) than UV treatment.

While the IR-induced association between TIP49b and ATF2 coincided with elevated ATF2 phosphorylation at the 1-h time point, at later times ATF2 phosphorylation decreased (Fig. 2C), suggesting that phosphorylation may be required to enable association, whereas another cellular mechanism(s) may regulate the dissociation of this complex. To directly assess the role of ATF2 phosphorylation in ATF2-TIP49b association, we expressed the constitutively active forms of p38 kinase (MKK6-DD) (13) or its upstream kinase ASK1 (ΔN-ASK1) (63). Both p38 upstream kinases efficiently induced ATF2 phosphorylation and led to a substantial increase in the association of TIP49b with ATF2 (Fig. 2D). Forced expression of ATF2 mutated on both phosphoacceptor sites revealed a weak association with TIP49b that did not increase after UV treatment or MKK6-DD expression (Fig. 2E). These observations provide direct evidence to support the conclusion that the association of TIP49b with ATF2 is phosphorylation dependent and is elevated following IR or UV irradiation.

TIP49b association with ATF2 attenuates ATF2 transcriptional activities. To assess the biological implications of the TIP49b-ATF2 association, we first monitored possible changes in ATF2 transcriptional activities. Using a luciferase reporter gene controlled by ATF2 target sequences (5xJun2-tk-luciferase construct [69]), we assessed changes in ATF2 transcriptional activities upon expression of TIP49b. Ectopic expression of TIP49b in HEK 293T cells led to a threefold decrease in the basal transcriptional activities of ATF2 (Fig. 3A). Changes in ATF2 transcriptional activities were not altered by exogenous expression of ATF2, suggesting that the amount of ATF2 in these reactions was not the limiting factor. A substantial increase (6- to 8-fold) in ATF2 transcriptional activities was observed after UV irradiation or IR, which was efficiently attenuated by TIP49b expression. p38 kinases (ΔN-ASK1 or MKK6-DD) elicited even stronger increase of ATF2 transcriptional activities (10- to 12-fold), which were as efficiently inhibited by TIP49b (Fig. 3A). These findings suggest that the association of TIP49b with ATF2 serves to limit basal and inducible transcriptional activities of ATF2.

Further analysis was carried out using the promoter of TNF-α, which contains a cyclic AMP (cAMP) response element (CRE), a target sequence for binding of ATF2/Jun heterodimers (68). Earlier studies had revealed the role of ATF2 in regulating of TNF-α transcription (33). Forced expression of TIP49b decreased basal as well as UV- or p38-inducible activation of −615 TNF-α–Luc (4- to 7-fold; Fig. 3B). TIP49b did not have any effect on TNF-α promoter mutated on the CRE (−615 TNF-α [mutCRE]-Luc [59]), confirming that the effect of TIP49b on TNF-α transcription is mediated through attenuation of ATF2 activities (Fig. 3B). These observations further establish that ATF2 transcriptional activities are suppressed under conditions that promote association with TIP49b.

To further elucidate the regulation of ATF2 transcriptional activities by TIP49b, we used normal and ATF2-null fibroblasts ($ATF2^{-/-}$). In contrast to its effect on ATF2 activities in normal human fibroblasts ($ATF2^{+/+}$), TIP49b did not affect transcription in fibroblasts lacking ATF2 (Fig. 3C). These data directly support the hypothesis that changes in the activities of CRE-based promoters seen upon expression of TIP49b are mediated via ATF2.

We further assessed whether TIP49a, which was not found to associate with ATF2, may alter ATF2 transcriptional activities. Forced expression of TIP49a did not alter basal or p38-inducible CRE-Luc activities, suggesting that TIP49a does not affect ATF2-mediated transcription. Like TIP49a, TIP49a-DN was not capable of altering ATF2 transcriptional output (Fig. 3D). These data suggest that TIP49a neither binds to ATF2 nor affects its transcriptional activities. Conversely, TIP49b-DN, which is mutated within the Walker B region implicated in its ATPase activity, was as effective as the wild-type form of TIP49b in attenuating both basal and inducible transcriptional activities of ATF2. These results suggest that the repression of ATF2 transcriptional activity is TIP49b specific and independent of ATPase or helicase activities. The latter is consistent with the notion that helicase activities may require the complex of both TIP49 proteins, which is not found to be associated with ATF2.

Given that the C-terminal domain of TIP49b is required for ATF2 association (Fig. 1E), we next assessed whether overexpression of this domain would alter ATF2 transcription. TIP49b-CT but not TIP49b-ΔC was capable of attenuating ATF2 transcriptional activity (Fig. 3E), suggesting that the C-terminal region of TIP49b is sufficient for interaction with and repression of ATF2 transcriptional activities. However, the interaction with and repression of ATF2 by TIP49b-CT were less efficient than with the wild-type protein, which implies that full-length TIP49b is needed for an efficient effect on ATF2.

Mapping the ATF2 domain required for interaction with TIP49b. We tested the possibility that the ATF2 domain required for association with TIP49b is within aa 150 to 248, since ATF2 from which this region has been deleted was not capable of associating with TIP49b (Fig. 1A) and since ATF2 Δ1–196 was still capable of associating with TIP49b in yeast two-hybrid assays (data not shown). Of interest, a naturally occurring splice form of ATF2 that lacks aa 150 to 248 is constitutively active transcriptionally (23).

To determine whether this is the domain required for association with TIP49b, we cloned aa 150 to 248 and aa 200 to 248 of ATF2 in frame with green fluorescent protein (GFP) and the penetratin sequence led by an HA tag into a mammalian expression vector (HA-$ATF2^{150–248}$-GFP). Of these two peptides, the one encompassing aa 150 to 248 of ATF2 exhibited greater expression levels and was chosen for further characterization.

Fluorescent microscopy-based analysis confirmed the expression and nuclear localization of the HA-$ATF2^{150–248}$-GFP construct (Fig. 4A, left panel). A direct interaction between the ATF2-driven aa 150 to 248 domain and TIP49b was revealed by the finding of HA-$ATF2^{150–248}$-GFP in Flag-TIP49b immunoprecipitates (Fig. 4A, right panel). Forced expression of

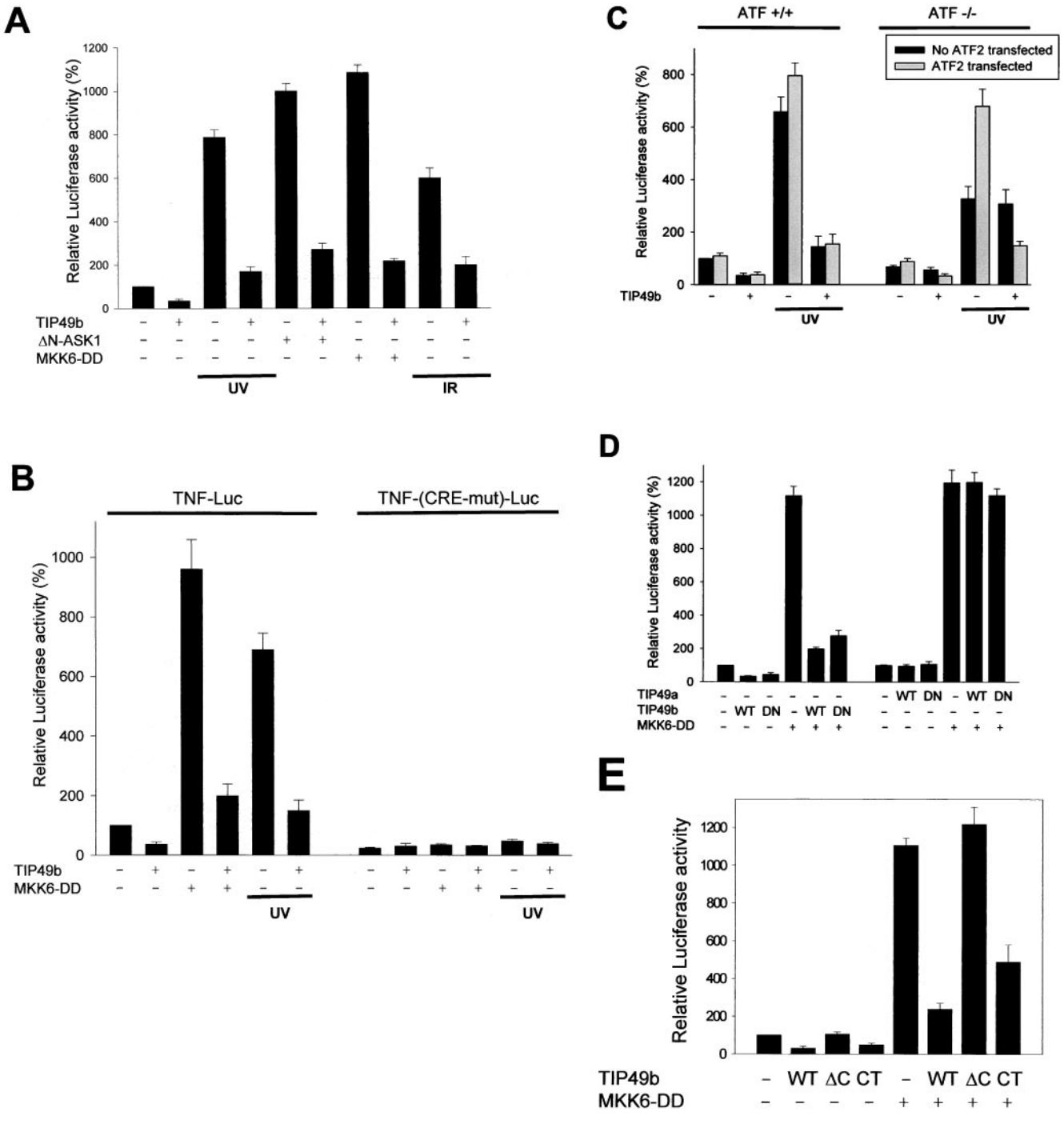

FIG. 3. TIP49b downregulates ATF2-dependent transcriptional activity. (A) 293T cells were transiently cotransfected with Flag-TIP49b, HA-ATF2, and MKK6-DD constructs as indicated, together with pCMV-β-gal and the reporter construct 5xJun2-tk-Luc. At 36 h after transfection, cells were treated with UV irradiation (60 J/m^2) or X-ray (5 Gy), and 6 h later cell lysates were prepared and assayed for luciferase and β-galactosidase activities. Luciferase activities were normalized to the β-galactosidase activities in the respective samples. Percent activities were calculated based on the control sample (5xJun2-tk-Luc alone). Data shown represent results from three experiments. (B) Experiments performed as for panel A were performed using TNF-Luc or TNF-(mutCRE)-Luc constructs as reporter plasmids. (C) Same luciferase assay experiments were performed using normal (ATF2$^{+/+}$) or ATF2-null (ATF2$^{-/-}$) fibroblasts. (D) ATF2$^{+/+}$ cells were cotransfected with wild-type Flag-TIP49a (WT) or domain mutated on D302N (DN) Flag-TIP49b (wild type [WT] or mutant [D299N]) and MKK6-DD constructs as indicated, together with pCMV-β-gal and 5xJun2-tk-Luc. (E) ATF2$^{+/+}$ cells were cotransfected with wild-type Flag-TIP49b (WT) or mutant ΔC (aa 1 to 306) or CT (aa 307 to 463) and MKK6-DD constructs as indicated, together with pCMV-β-gal and 5xJun2-tk-Luc.

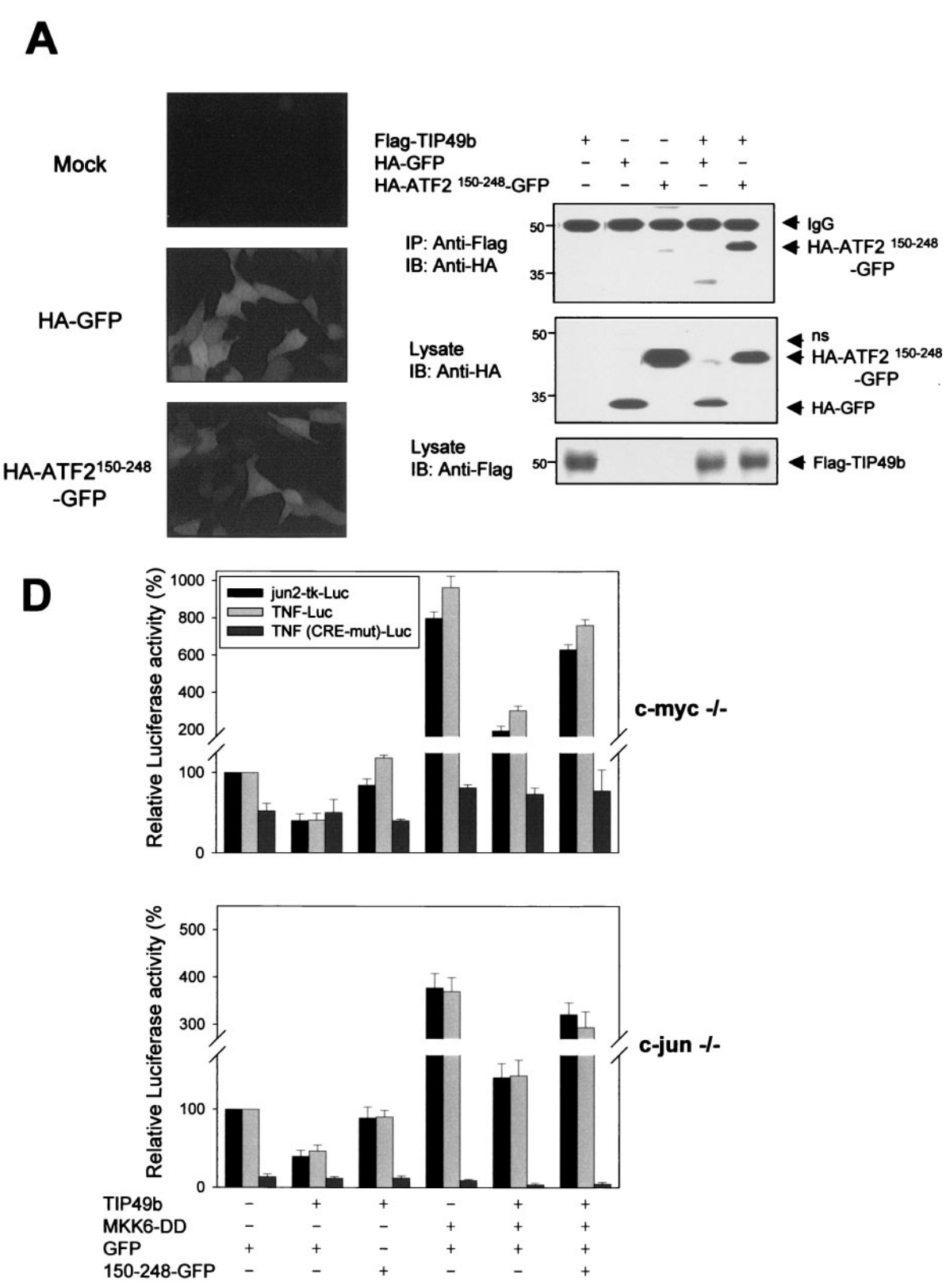

FIG. 4. Expression of ATF2$^{150–248}$ attenuated the interaction between ATF2 and TIP49b specifically. (A) Normal fibroblasts were transiently transfected with HA-ATF2$^{150–248}$-GFP (or its control construct, HA-GFP) as indicated, and 36 h later, the expression of the constructs was confirmed under fluorescent microscopy (left). Cells were cotransfected with Flag-TIP49b and HA-ATF2$^{150–248}$-GFP, and lysates were immunoprecipitated (IP) with anti-Flag antibody. The bottom panels verify expression of the exogenously expressed proteins (right). (B) Cells were cotransfected with Flag-TIP496, HA-ATF2$^{150–248}$-GFP, and ΔN-ASK1, and lysates were immunoprecipitated with anti-Flag antibodies. The immunoprecipitates or lysates were immunoblotted (IB) with the indicted antibodies. (C and D) ATF2$^{+/+}$, ATF2$^{-/-}$, c-Myc$^{-/-}$, and c-Jun$^{-/-}$ cells were cotransfected with Flag-TIP49b, MKK6-DD, HA-ATF2, and HA-ATF2$^{150–248}$-GFP (or HA-GFP) constructs as indicated, together with pCMV-β-gal and the reporter construct (5xJun2-tk-Luc, TNF-Luc, or TNF-[mutCRE]-Luc). Lysates were assayed for luciferase and β-galactosidase activities as indicated above.

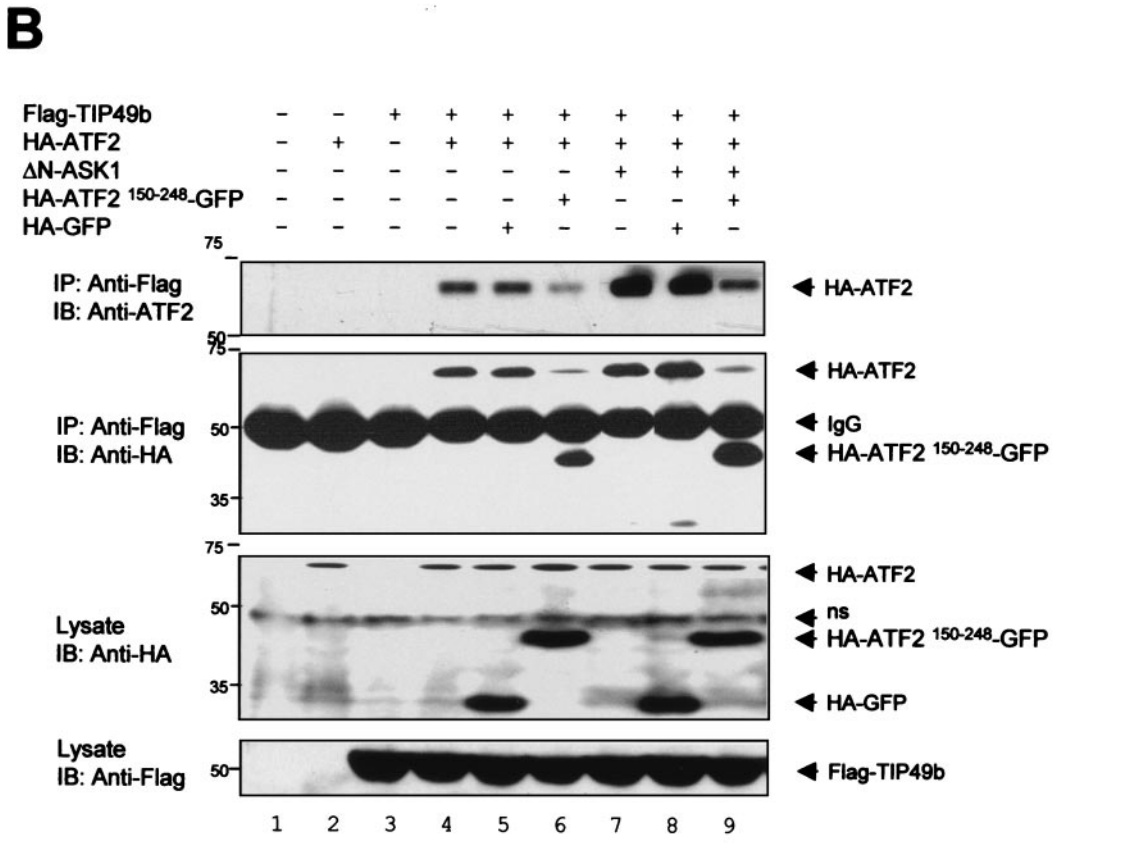

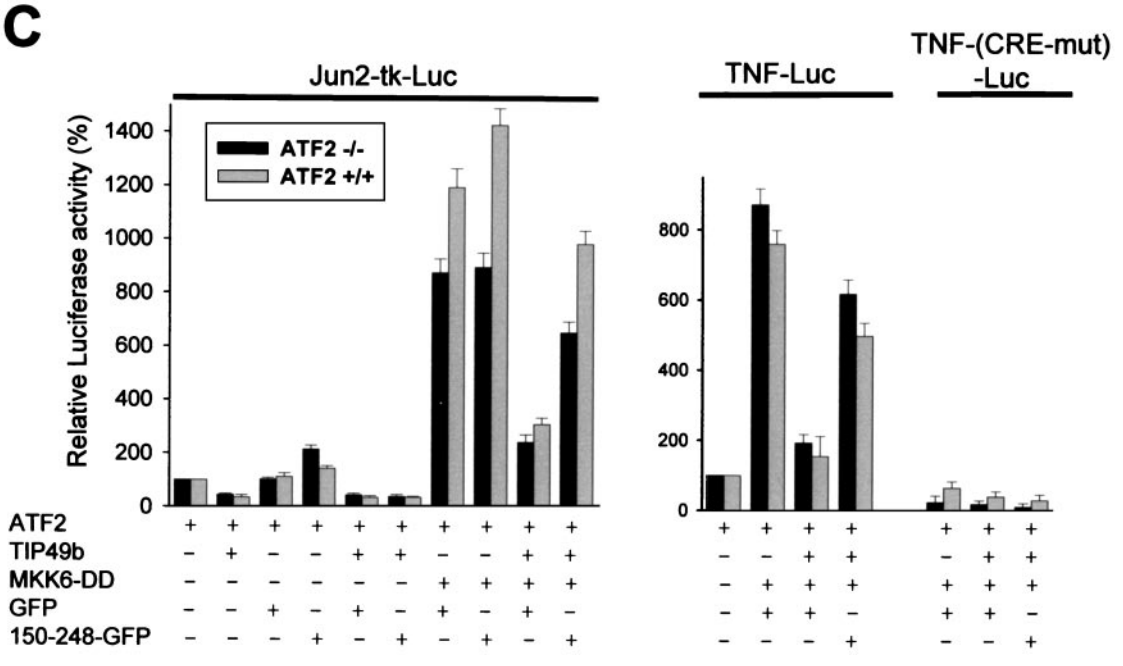

FIG. 4—*Continued.*

TIP49b and ATF2 in normal human fibroblasts revealed the association between the two proteins (Fig. 4B, lane 4), which increased upon ΔN-ASK1 expression (lane 7).

Coexpression of HA-ATF2$^{150–248}$-GFP led to a marked decrease in the association of TIP49b with full-length ATF2 (Fig. 4B, lanes 6 and 9), whereas the control construct (HA-GFP) did not alter this interaction (lanes 5 and 8). Forced expression of HA-ATF2$^{150–248}$-GFP efficiently inhibited both basal and

p38-inducible association of ATF2 with TIP49b (Fig. 4B). These results suggest that the domain corresponding to amino acids 150 to 248 encompasses the ATF2 region that is required for association with TIP49b and for the ability to outcompete the association between ATF2 and TIP49b upon overexpression of this domain.

Inhibition of the TIP49b-ATF2 association was reflected at the level of ATF2 transcriptional activities. Forced expression of HA-ATF2$^{150–248}$-GFP increased the basal level of ATF2 transcription both in normal fibroblasts and in ATF2-null fibroblasts supplemented with exogenous ATF2 (Fig. 4C). No changes were observed in ATF2 transcriptional activity upon expression of the HA-ATF2$^{150–248}$-GFP construct in ATF2-null cells without providing exogenous ATF2 (data not shown). Whereas expression of HA-ATF2$^{150–248}$-GFP did not affect the p38-mediated increase in ATF2 transcriptional activities, coexpression of TIP49b inhibited the p38-mediated increase in ATF2 transcription; such inhibition was attenuated upon expression of HA-ATF2$^{150–248}$-GFP (Fig. 4C). Similar observations were made using the TNF-α promoter sequences but not a CRE mutant-bearing promoter (Fig. 4C). These data suggest that the inhibition of the ATF2-TIP49b association by the competing ATF2-driven peptide sufficed to attenuate the inhibition of ATF2 transcriptional activities by TIP49b.

Ability of ATF2$^{150–248}$ to attenuate repression of TIP49b on ATF2-mediated transcription is ATF2 specific. TIP49a and TIP49b were recently shown to associate with c-Myc. TIP49a functions as a positive cofactor of Myc-mediated oncogenic transformation (73). Given the ability of c-Myc to associate with both TIP49 components, we assessed whether the effects of TIP49b on ATF2 are Myc dependent. To this end, we tested TIP49b's ability to silence ATF2 transcriptional activities in c-Myc$^{-/-}$ cells. Forced expression of TIP49b resulted in suppression of basal and, more so, of p38-induced ATF2 transcriptional activities, monitored via Jun2-Luc and TNF-α–Luc, in a fashion similar to that observed in the c-Myc-positive cells (Fig. 4D). These results support the notion that c-Myc is not required for TIP49b's ability to suppress ATF2-mediated transcription.

Since c-Jun is among the key ATF2 heterodimerizing partners, we next assessed whether TIP49b maintains its inhibitory effects on ATF2 transcription in a c-Jun-null environment. Coexpression of ATF2 and TIP49b in c-*jun*$^{-/-}$ cells revealed TIP49b-mediated repression, which was also efficient after p38 activation, similar to that observation in normal human fibroblasts. Expression of the ATF2$^{150–248}$ peptide efficiently attenuated TIP49b-mediated suppression of p38-induced ATF2 transcriptional activities (Fig. 4D).

β-Catenin, an important member of the Wnt signaling cascade, was also reported to interact with TIP49a (4) and TIP49b (3). Whereas TIP49a activated β-catenin transcriptional activities, TIP49b repressed them (3). In view of these findings, we assessed whether the ATF2$^{150–248}$ peptide would affect β-catenin-mediated transcription. Coexpression of TIP49b, β-catenin^{S33Y} (the S33Y mutant lacks one of the glycogen synthase kinase 3β (GSK3β) phosphorylation sites, rendering it insusceptible to homologue of Slimb (HOS)/GSK3β-mediated degradation [22]), and the TOPFLASH luciferase construct (which contains five TCF binding sites [42]) efficiently decreased the degree of TCF transactivation, which could not be attenuated upon coexpression of the ATF2$^{150–248}$ peptide (data not shown). These results suggest that the effect elicited by ATF2$^{150–248}$ is specific to ATF2 and does not require or alter activities of other TIP49b-associated factors, as shown here for c-Myc and β-catenin.

Constitutive expression of ATF2$^{150–248}$ peptide alters ATF2 transcription, cell cycle distribution, and degree of cell death in response to irradiation. To further evaluate the biological implications of altered ATF2 transcription, we established ATF2$^{+/+}$ and ATF2$^{-/-}$ fibroblast cells, as well as a melanoma-derived cell line, K1735p (55), which constitutively expresses the ATF2$^{150–248}$ peptide. The expression of ATF2$^{150–248}$ in nuclei of transfected cells was confirmed by fluorescence microscopy (Fig. 5A) as well as via Western blotting (Fig. 5B). Cells that constitutively express the ATF2$^{150–248}$ peptide revealed a marked decrease in the association between TIP49b and ATF2 under normal growth conditions and more so following UV or IR treatment (Fig. 5B).

Decreased association between the ATF2 and TIP49b was also reflected at the level of ATF2 transcriptional activities. Cells that constitutively express the ATF2$^{150–248}$ peptide exhibited an elevated degree of ATF2 transcriptional activities under normal growth conditions as well as after exposure to UV or IR treatment (Fig. 5C). Similar observations were made using the Jun2-tk-Luc reporter construct (data not shown). Conversely, expression of the ATF2 peptide did not alter the level of TCF-mediated transcription (Fig. 5C). While providing important support for the specific effect of the ATF2 peptide on TIP49b-mediated inhibition of ATF2 transcriptional activities, these results also indicate that the nature of the TIP49b association with ATF2 serves primarily to limit the degree of ATF2 transcriptional output.

Following confirmation of the ability of the ATF2 peptide to attenuate ATF2 association with and inhibition by TIP49b, we elucidated possible changes in the cells' ability to cope with stress conditions, which are known to activate ATF2. Under normal growth conditions, none of the three cell lines that constitutively express ATF2$^{150–248}$ was found to exhibit altered cell cycle distribution. However, substantial changes were found following IR of human fibroblasts and melanoma cells but not of ATF2-null fibroblasts (Fig. 6). Similar data were observed after UV irradiation (data not shown).

Changes seen after irradiation can be divided into two stages. First, as early as 6 h and to a greater extent 12 h after UV irradiation, there was a noticeable increase (32 to 50%) in the fraction of cells found in the G_2M phase of the cell cycle (data not shown). A similar change was observed following IR (Fig. 6). At a later time after irradiation (48 h) there was a marked increase (up to 3-fold) in the fraction of cells that were found in the sub-G_1 phase that reflects apoptosis (Fig. 6, and data not shown). The increased fraction of cells undergoing apoptosis as seen following UV or IR treatment suggests that ATF2 may elicit a proapoptotic signal under stress conditions, depending on the degree of TIP49b inhibition.

DISCUSSION

The present study demonstrates the association of TIP49b with ATF2 and the biological implications of this association. ATF2's association with TIP49b takes place in normal growing

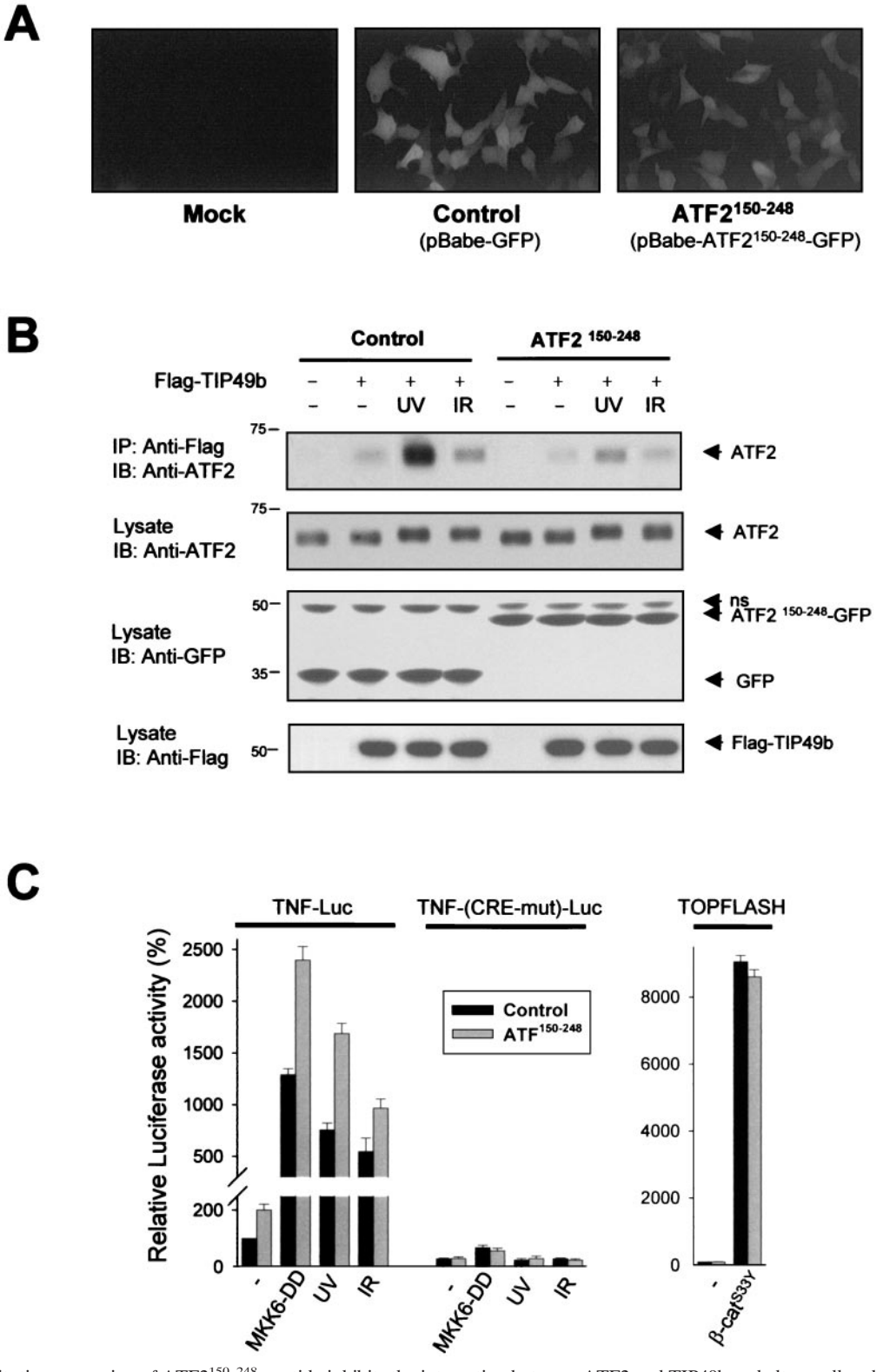

FIG. 5. Constitutive expression of ATF2$^{150–248}$ peptide inhibits the interaction between ATF2 and TIP49b and alters cell cycle distribution and apoptosis following radiation. Retroviral construct pBabe-ATF2$^{150–248}$-GFP and its control construct pBabe-GFP were used to transfect packaging cells, and the retroviral supernatants were infected into normal human fibroblasts (ATF2$^{+/+}$), ATF2$^{-/-}$ cells, and melanoma K1735p cells (55). (A) Expression of the constructs in ATF2$^{+/+}$ cells was analyzed by fluorescent microscopy. (B) Control and ATF2$^{150–248}$-expressing cells were transfected with Flag-TIP49b, and 36 h later, the cells were irradiated with UV or X-rays. Cell lysates were immunoprecipitated with anti-Flag antibody and immunoblotted with anti-ATF2 antibody. The bottom panels depict expression of the exogenously expressed proteins. (C) Control and ATF2$^{150–248}$-expressing cells were transfected with pCMV-β-gal and the reporter construct (TNF-Luc, TNF-[mutCRE]-Luc, or TOPFLASH) together with MKK6-DD or β-cat^{S33Y}, as indicated. After 36 h, the indicated cells were treated with UV or X-rays. Cell lysates were used for luciferase and β-galactosidase assays.

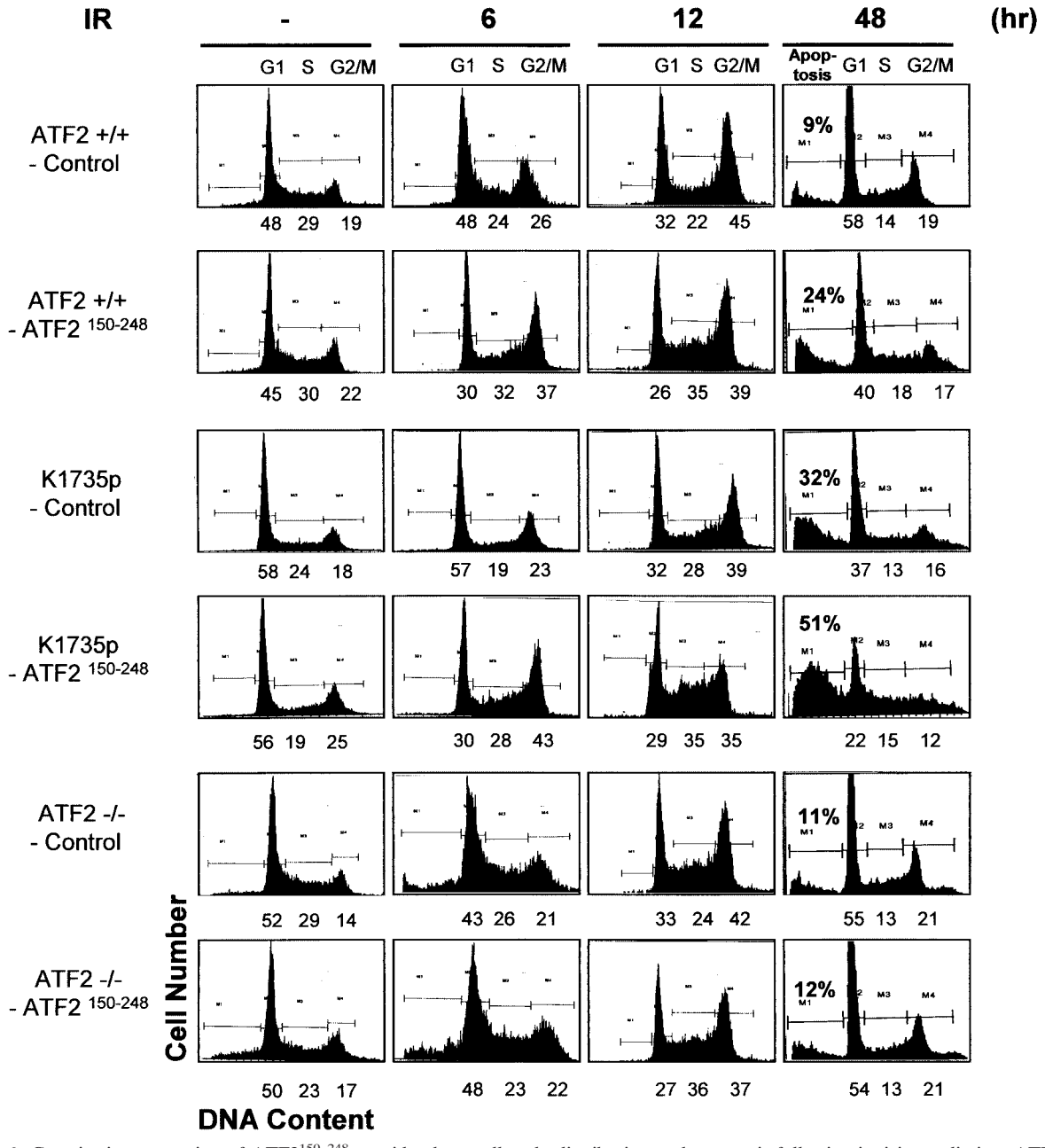

FIG. 6. Constitutive expression of ATF2$^{150–248}$ peptide alters cell cycle distribution and apoptosis following ionizing radiation. ATF2$^{150–248}$-expressing fibroblasts, K1735p melanoma cells, and ATF2-null cells were exposed to IR, and their apoptotic and cell cycle profiles were determined by fluorescence-activated cell sorter analysis at the indicated time points.

cells; the association is more pronounced following exposure to treatments that induce ATF2 phosphorylation, which is required for ATF2 transcriptional activities. Our findings suggest that the TIP49b association with ATF2 is a mechanism that serves to limit ATF2 transcriptional activities. Accordingly, the association of ATF2 with TIP49b highlights a novel layer of regulation for ATF2 transcriptional activities.

The nature of ATF2 regulation by TIP49b suggests that ATF2 plays an important role in the cell's response to stress. Support for this notion comes from experiments in which we successfully outcompeted the TIP49b-ATF2 association by overexpression of the ATF2 peptide corresponding to the ATF2 domain required for the association with TIP49b. As a result of increased ATF2 transcriptional output, there was a marked change in the cell's response to stress and DNA damage.

Irradiation of fibroblasts as well as melanoma cells in which the TIP49b association with ATF2 was impaired resulted in an elevated fraction of cells found in the G_2M phase of the cell cycle within 6 to 12 h after treatment. This finding suggests that ATF2 may regulate an inhibitor of G_2M exit or regulator of cell entry into mitosis. Alternatively, ATF2 may affect a protein that potentiates the exit from S phase to G_2M. Ongoing studies are aimed at addressing each of these possibilities. The altered cell cycle distribution observed in response to treatment by IR

or UV further corroborates the role of the ATF2-TIP49b association in cell cycle control.

Release of ATF2 transcriptional output from TIP49b-mediated restriction also resulted in an increased degree of apoptosis induced by irradiation, pointing to the role of ATF2 in the induction of programmed cell death. The latter is in line with our earlier studies in which we demonstrated that ATF2 contributes to the apoptosis of early- but not late-stage melanoma cells due to upregulation of TNF-α, which elicits the primary apoptotic signal in early melanomas (33). Given that the K1735p melanoma cells used in the present study represent early-stage melanoma cells and that the same changes were also observed in nontransformed fibroblasts, we suggest that ATF2 may serve to potentiate apoptosis in response to DNA damage, as shown here for UV and IR. It is the level of TIP49b, as well as the degree of ATF2 phosphorylation, which is expected to dictate the amount of ATF2-TIP49b complex and concomitant ability of ATF2 to elicit a proapoptotic signal.

The mechanism underlying TIP49b's ability to alter ATF2 activities may relate to its role in the chromatin-remodeling complex (1, 34, 74). TIP49b was originally identified as a TATA-binding protein (TBP)-interacting protein (35) and is among 12 polypeptides that compose the INO80 chromatin-remodeling complex. While exhibiting DNA-dependent ATPase activity, INO80 chromatin remodeling has been implicated in both transcription and DNA damage repair (65). Through its effects on potential Holliday junction intermediates, the RuvAB complex (RuvB is a TIP49b homologue) prevents double-strand breaks at arrested replication forks (64).

The recent findings that RuvB-like proteins are part of the multisubunit TIP60 HAT complex (31) further point to their role in diverse functions associated with chromatin metabolism. Along these lines, association of ATF2 with TIP49b appears to be required for its ability to mediate DNA repair of double-strand breaks, since inhibition of such association impairs double-strand break repair after IR (data not shown). That the TIP49b-ATF2 association results in inhibition of ATF2 transcription also implies that other components of the chromatin-remodeling complex may be affected upon TIP49 association, resulting in impaired transcription.

Our observations are in line with the notion that TIP49b elicits inhibition of c-Myc and β-catenin transcription. It is also possible that the changes observed in cell cycle and apoptosis are not only TIP49b related, since other ATF2-associated proteins may be outcompeted by the peptide corresponding to aa 150 to 249. Although there are no reports on ATF2 binding proteins within this region, we cannot exclude this possibility completely because of the correlation between the changes seen in and TIP49b dissociation with ATF2.

The TIP49b effect on ATF2 transcriptional activities may also be elicited via altered ATF2 HAT activities. UV treatment or ATF2 phosphorylation increases its HAT as well as its transcriptional activities (38). Of interest, inhibition of histone deacetylases triggers a G_2-phase cell cycle checkpoint response in normal human cells but not in tumor cells (7), which further points to a possible link between ATF2 HAT activities and its effects on G_2M arrest following DNA damage.

Our data cannot exclude the possibility that TIP49b may also affect ATF2 transcriptional activities via masking the transactivation domain from binding to some other nuclear cofactors. Unlike ATF2, where only TIP49b was found as an associated protein, both c-Myc and β-catenin were shown to associate with both TIP49 components. Importantly, whereas TIP49b elicits suppression of transcriptional activities of proteins to which it binds, TIP49a amplifies the transcriptional output of its bound transcription factors (4, 73).

It is important to emphasize that the effect of TIP49b on ATF2 is selective, specific, and dissociated from its effects on other key regulatory proteins, as shown for c-Myc and β-catenin.

The distinct difference in the nature of the selective ATF2 association with TIP49b is in line with the principal difference in the types of activities mediated by ATF2, as opposed to transcription factors associated with TIP49a. Whereas ATF2 emerges as an inhibitor of the cell cycle and induces apoptosis in response to DNA damage, both c-Myc and β-catenin potentiate growth, replication, and transformation. The latter may explain why cells will not favor unrestricted ATF2 activities but rather tightly limit ATF2 transcriptional output.

ACKNOWLEDGMENTS

We thank Kazunari Yokoyama for ATF2-null cells, Ron Wisdom for Jun-null cells, John Sedivy for Myc-null cells, Laurie Owen Schaub for K1735p melanoma cells, Hidetoshi Tahara for normal human fibroblasts, and Garry Nolan for the Phoenix cells. We also thank M. Cole, M. Karin, R. Davis, and H. Ichijo for TIP49/MAPK/JNK/p38 constructs and T. Tamura for the antibodies to TIP49b. We thank members of the Ronai lab for discussions.

Support from NCI grant CA59905 (to Z.R.) is gratefully acknowledged.

REFERENCES

1. **Armstrong, J. A., and B. M. Emerson.** 1998. Transcription of chromatin: these are complex times. Curr. Opin. Genet. Dev. **8:**165–172.
2. **Badie, C., G. Iliakis, N. Foray, G. Alsbeih, B. Cedervall, N. Chavaudra, G. Pantelias, C. Arlett, and E. P. Malaise.** 1995. Induction and rejoining of DNA double-strand breaks and interphase chromosome breaks after exposure to X rays in one normal and two hypersensitive human fibroblast cell lines. Radiat. Res. **144:**26–35.
3. **Bauer, A., S. Chauvet, O. Huber, F. Usseglio, U. Rothbacher, D. Aragnol, R. Kemler, and J. Pradel.** 2000. Pontin52 and reptin52 function as antagonistic regulators of beta-catenin signalling activity. EMBO J. **19:**6121–6130.
4. **Bauer, A., O. Huber, and R. Kemler.** 1998. Pontin52, an interaction partner of beta-catenin, binds to the TATA box binding protein. Proc. Natl. Acad. Sci. USA **95:**14787–14792.
5. **Bender, K., C. Blattner, A. Knebel, M. Iordanov, P. Herrlich, and H. J. Rahmsdorf.** 1997. UV-induced signal transduction. J. Photochem. Photobiol. B. **37:**1–17.
6. **Bhoumik, A., V. Ivanov, and Z. Ronai.** 2001. Activating transcription factor 2-derived peptides alter resistance of human tumor cell lines to ultraviolet irradiation and chemical treatment. Clin. Cancer Res. **7:**331–342.
7. **Burgess, S. M., M. Ajimura, and N. Kleckner.** 1999. GCN5-dependent histone H3 acetylation and RPD3-dependent histone H4 deacetylation have distinct, opposing effects on IME2 transcription, during meiosis and during vegetative growth, in budding yeast. Proc. Natl. Acad. Sci. USA **96:**6835–6840.
8. **Cairns, B. R., Y. Lorch, Y. Li, M. Zhang, L. Lacomis, H. Erdjument-Bromage, P. Tempst, J. Du, B. Laurent, and R. D. Kornberg.** 1996. RSC, an essential, abundant chromatin-remodeling complex. Cell **87:**1249–1260.
9. **Cantor, S. B., D. W. Bell, S. Ganesan, E. M. Kass, R. Drapkin, S. Grossman, D. C. Wahrer, D. C. Sgroi, W. S. Lane, D. A. Haber, and D. M. Livingston.** 2001. BACH1, a novel helicase-like protein, interacts directly with BRCA1 and contributes to its DNA repair function. Cell **105:**149–160.
10. **Chatton, B., J. L. Bocco, J. Goetz, M. Gaire, Y. Lutz, and C. Kedinger.** 1994. Jun and Fos heterodimerize with ATFa, a member of the ATF/CREB family and modulate its transcriptional activity. Oncogene **9:**375–385.
11. **Chatton, B., J. L. Bocco, M. Gaire, C. Hauss, B. Reimund, J. Goetz, and C. Kedinger.** 1993. Transcriptional activation by the adenovirus larger E1a product is mediated by members of the cellular transcriptional factor ATF family which can directly associate with E1a. Mol. Cell. Biol. **13:**561–570.
12. **Chen, C., and H. Okayama.** 1987. High-efficiency transformation of mam-

malian cells by plasmid DNA. Mol. Cell. Biol. **7:**2745–2752.
13. **Chen, C. Y., F. Del Gatto-Konczak, Z. Wu, and M. Karin.** 1998. Stabilization of interleukin-2 mRNA by the c-Jun NH_2-terminal kinase pathway. Science **280:**1945–1949.
14. **Clerk, A., and P. H. Sugden.** 1997. Cell stress-induced phosphorylation of ATF2 and c-Jun transcription factors in rat ventricular myocytes. Biochem. J. **325:**801–810.
15. **Cote, J., J. Quinn, J. L. Workman, and C. L. Peterson.** 1994. Stimulation of GAL4 derivative binding to nucleosomal DNA by the yeast SWI/SNF complex. Science **265:**53–60.
16. **Crowe, D. L., and B. Shemirani.** 2000. The transcription factor ATF-2 inhibits extracellular signal regulated kinase expression and proliferation of human cancer cells. Anticancer Res. **20:**2945–2949.
17. **De Cesare, D., D. Vallone, A. Caracciolo, P. Sassone-Corsi, C. Nerlov, and P. Verde.** 1995. Heterodimerization of c-Jun with ATF-2 and c-Fos is required for positive and negative regulation of the human urokinase enhancer. Oncogene **11:**365–376.
18. **Derijard, B., M. Hibi, H.-I. Wu, T. Barret, B. Su, T. Deng, M. Karin, and R. Davis.** 1994. JNK1: a protein kinase stimulated by UV light and Ha-Ras that binds and phosphorylates the c-Jun activation domain. Cell **76:**1025–1037.
19. **Du, W., D. Thanos, and T. Maniatis.** 1993. Mechanisms of transcriptional synergism between distinct virus-inducible enhancer elements. Cell **74:**887–898.
20. **Duyndam, M. C. A., H. van Dam, A. J. van der Eb, and A. Zantema.** 1996. The CR1 and CR3 domains of the adenovirus type 4 E1A proteins can independently mediate activation of ATF-2. J. Virol. **70:**5852–5959.
21. **Flint, K. J., and N. C. Jones.** 1991. Differential regulation of three members of the ATF/CREB family of DNA-binding proteins. Oncogene **6:**2019–2026.
22. **Fuchs, S. Y., A. Chen, Y. Xiong, Z. Q. Pan, and Z. Ronai.** 1999. HOS, a human homolog of Slimb, forms an SCF complex with Skp1 and Cullin1 and targets the phosphorylation-dependent degradation of IκB and beta-catenin. Oncogene **18:**2039–2046.
23. **Georgopoulos, K., K. B. Morgan, and D. D. Moore.** 1992. Functionally distinct isoforms of the CRE-BP DNA-binding protein mediate activity of a T-cell-specific enhancer. Mol. Cell. Biol. **12:**747–757.
24. **Gohshi, T., M. Shimada, S. Kawahire, N. Imai, T. Ichimura, S. Omata, and T. Horigome.** 1999. Molecular cloning of mouse p47, a second group mammalian RuvB DNA helicase-like protein: homology with those from human and *Saccharomyces cerevisiae*. J. Biochem. **125:**939–946.
25. **Gupta, S., D. Campbell, B. Derijard, and R. J. Davis.** 1995. Transcription factor ATF-2 regulation by the JNK signal transduction pathway. Science **276:**389–393.
26. **Hagmeyer, B. M., H. Konig, I. Herr, R. Offringa, A. Zantema, A. van der Eb, P. Herrlich, and P. Angel.** 1993. Adenovirus E1A negatively and positively modulates transcription of AP-1 dependent genes by dimer-specific regulation of the DNA binding and transactivation activities of Jun. EMBO J. **12:**3559–3572.
27. **Hai, T., and T. Curran.** 1991. Cross-family dimerization of transcription factors Fos/Jun and ATF/CREB alters DNA binding specificity. Proc. Natl. Acad. Sci. USA **88:**3720–3724.
28. **Hai, T., F. Liu, W. J. Coukos, and M. R. Green.** 1989. Transcription factor ATF cDNA clones: an extensive family of leucine aipper proteins able to selectively form DNA-binding heterodimers. Genes Dev. **3:**2083–2090.
29. **Holzmann, K., C. Gerner, T. Korosec, A. Poltl, R. Grimm, and G. Sauermann.** 1998. Identification and characterization of the ubiquitously occurring nuclear matrix protein NMP 238. Biochem. Biophys. Res. Commun. **252:**39–45.
30. **Huguier, S., J. Baguet, S. Perez, H. van Dam, and M. Castellazzi.** 1998. Transcription factor ATF2 cooperates with v-Jun to promote growth factor-independent proliferation in vitro and tumor formation in vivo. Mol. Cell. Biol. **18:**7020–7029.
31. **Ikura, T., V. V. Ogryzko, M. Grigoriev, R. Groisman, J. Wang, M. Horikoshi, R. Scully, J. Qin, and Y. Nakatani.** 2000. Involvement of the TIP60 histone acetylase complex in DNA repair and apoptosis. Cell **102:**463–474.
32. **Ivanov, V. N., O. Fodstad, and Z. Ronai.** 2001. Expression of ring finger-deleted TRAF2 sensitizes metastatic melanoma cells to apoptosis via up-regulation of p38, TNFalpha and suppression of NF-kappaB activities. Oncogene **20:**2243–2253.
33. **Ivanov, V. N., and Z. Ronai.** 1999. Down-regulation of tumor necrosis factor alpha expression by activating transcription factor 2 increases UVC-induced apoptosis of late-stage melanoma cells. J. Biol. Chem. **274:**14079–14089.
34. **Kadonaga, J. T.** 1998. Eukaryotic transcription: an interlaced network of transcription factors and chromatin-modifying machines. Cell **92:**307–313.
35. **Kanemaki, M., Y. Kurokawa, T. Matsu-ura, Y. Makino, A. Masani, K. Okazaki, T. Morishita, and T. A. Tamura.** 1999. TIP49b, a new RuvB-like DNA helicase, is included in a complex together with another RuvB-like DNA helicase, TIP49a. J. Biol. Chem. **274:**22437–22444.
36. **Kanemaki, M., Y. Makino, T. Yoshida, T. Kishimoto, A. Koga, K. Yamamoto, M. Yamamoto, V. Moncollin, J. M. Egly, M. Muramatsu, and T. Tamura.** 1997. Molecular cloning of a rat 49-kDa TBP-interacting protein (TIP49) that is highly homologous to the bacterial RuvB. Biochem. Biophys. Res. Commun. **253:**64–68.
37. **Kashuba, V. I., R. Z. Gizatullin, A. I. Protopopov, R. Allikmets, S. Korolev, J. Li, F. Boldog, K. Tory, V. Zabarovska, Z. Marcsek, J. Sumegi, G. Klein, E. R. Zabarovsky, and L. Kisselev.** 1997. NotI linking/jumping clones of human chromosome 3: mapping of the TFRC, RAB7 and HAUSP genes to regions rearranged in leukemia and deleted in solid tumors. FEBS Lett. **419:**181–185.
38. **Kawasaki, H., L. Schiltz, R. Chiu, K. Itakura, K. Taira, Y. Nakatani, and K. K. Yokoyama.** 2000. ATF-2 has intrinsic histone acetyltransferase activity which is modulated by phosphorylation. Nature **405:**195–200.
39. **Kawasaki, H., J. Song, R. Eckner, H. Ugai, R. Chiu K. Taira, Y. Shi, N. Jones, and K. K. Yokoyama.** 1998. p300 and ATF-2 are components of the DRF complex, which regulates retinoic acid- and E1A-mediated transcription of the c-jun gene in F9 cells. Genes Dev. **12:**233–245.
40. **Kikuchi, N., T. Gohshi, S. Kawahire, T. Tachibana, Y. Yoneda, T. Isobe, C. R. Lim, K. Kohno, T. Ichimura, S. Omata, and T. Horigome.** 1999. Molecular shape and ATP binding activity of rat p50, a putative mammalian homologue of RuvB DNA helicase. J. Biochem. **125:**487–494.
41. **Kim, S. J., S. Wagner, F. Liu, M. A. O'Reilly, P. D. Robbins, and M. R. Green.** 1992. Retinoblastoma gene product activates expression of the human TGF-beta 2 gene through transcriptional factor ATF-2. Nature **358:**331–334.
42. **Korinek, V., N. Barker, P. J. Morin, D. van Wichen, R. de Weger, K. W. Kinzler, B. Vogelstein, and H. Clevers.** 1997. Constitutive transcriptional activation by a beta-catenin-Tcf complex in APC−/− colon carcinoma. Science **275:**1784–1787.
43. **Li, X. Y., and M. R. Green.** 1996. Intramolecular inhibition of activating transcription factor-2 function by its DNA-binding domain. Genes Dev. **10:**517–527.
44. **Lim, C. R., Y. Kimata, H. Ohdate, T. Kokubo, N. Kikuchi, T. Horigome, and K. Kohno.** 2000. The Saccharomyces cerevisiae RuvB-like protein, Tih2p, is required for cell cycle progression and RNA polymerase II-directed transcription. J. Biol. Chem. **275:**22409–22417.
45. **Liu, F., and M. R. Green.** 1990. A specific member of the ATF transcription factor family can mediate transcription activation by the adenovirus E1a protein. Cell **61:**1217–1224.
46. **Liu, F., and M. R. Green.** 1994. Promoter targeting by adenovirus E1a through interaction with different cellular DNA-binding domains. Nature **368:**520–525.
47. **Livingston, C., G. Patel, and N. Jones.** 1995. ATF-2 contains a phosphorylation-dependent transcriptional activation domain. EMBO J. **14:**1785–1797.
48. **Maekawa, T., F. Bernier, M. Sato, S. Nomura, M. Singh, Y. Inoue, T. Tokunaga, H. Imai, M. Yokoyama, A. Reimold, L. H. Glimcher, and S. Ishii.** 1999. Mouse ATF-2 null mutants display features of a severe type of meconium aspiration syndrome. J. Biol. Chem. **274:**17813–17819.
49. **Maekawa, T., H. Sakura, C. Kanei-Ishii, T. Sudo, T. Yoshimura, J. Fujisawa, M. Yoshida, and S. Ishii.** 1989. Leucine zipper structure of the protein CRE-BP1 binding to the cyclic AMP response element in brain. EMBO J. **8:**2023–2028.
50. **Makino, Y., M. Kanemaki, A. Koga, K. Osano, T. Matsu-Ura, Y. Kurokawa, T. Kishimoto, and T. Tamura.** 2000. Chromosome mapping and expression of human tip49 family genes. DNA Sequence **11:**145–148.
51. **Makino, Y., M. Kanemaki, Y. Kurokawa, T. Koji, and T. A. Tamura.** 1999. A rat RuvB-like protein, TIP49a, is a germ cell-enriched novel DNA helicase. J. Biol. Chem. **274:**15329–15335.
52. **Mateyak, M. K., A. J. Obaya, S. Adachi, and J. M. Sedivy.** 1997. Phenotypes of c-Myc-deficient rat fibroblasts isolated by targeted homologous recombination. Cell Growth Differ. **8:**1039–1048.
53. **Mezard, C., A. A. Davies, A. Stasiak, and S. C. West.** 1997. Biochemical properties of RuvBD113N: a mutation in helicase motif II of the RuvB hexamer affects DNA binding and ATPase activities. J. Mol. Biol. **271:**704–717.
54. **Newell, C. L., A. B. Deisseroth, and G. Lopez-Berestein.** 1994. Interaction of nuclear proteins with an AP-1/CRE-like promoter sequence in the human TNF-α gene. J. Leukoc. Biol. **56:**27–35.
55. **Owen-Schaub, L. B., K. L. van Golen, L. L. Hill, and J. E. Price.** 1998. Fas and Fas ligand interactions suppress melanoma lung metastasis. J. Exp. Med. **188:**1717–1723.
56. **Parfait, B., Y. Giovangrandi, M. Asheuer, I. Laurendeau, M. Olivi, N. Vodovar, D. Vidaud, M. Vidaud, and I. Bieche.** 2000. Human TIP49b/RUVBL2 gene: genomic structure, expression pattern, physical link to the human CGB/LHB gene cluster on chromosome 19q13.3. Ann. Genet. **43:**69–74.
57. **Pear, W. S., G. P. Nolan, M. L. Scott, and D. Baltimore.** 1993. Production of high-titer helper-free retroviruses by transient transfection. Proc. Natl. Acad. Sci. USA **90:**8392–8396.
58. **Qiu, X. B., Y. L. Lin, K. C. Thome, P. Pian, B. P. Schlegel, S. Weremowicz, J. D. Parvin, and A. Dutta.** 1998. An eukaryotic RuvB-like protein (RUVBL1) essential for growth. J. Biol. Chem. **273:**27786–27793.
59. **Rhoades, K. L., S. H. Golub, and J. S. Economou.** 1992. The regulation of the human tumor necrosis factor alpha promoter region in macrophage, T cell, and B cell lines. J. Biol. Chem. **267:**22102–22107.
60. **Ronai, Z., Y. M. Yang, S. Y. Fuchs, V. Adler, M. Sardana, and M. Herlyn.**

1998. ATF2 confers radiation resistance to human melanoma cells. Oncogene **16:**523–531.
61. **Rutberg, S. E., Y. Yang, and Z. Ronai.** 1992. Functional role of the ultraviolet light responsive element (URE; TGACAACA) in the transcription and replication of polyoma DNA. Nucleic Acids Res. **16:**4305–4310.
62. **Rynditch, A., Y. Pekarsky, S. Schnittger, and K. Gardiner.** 1997. Leukemia breakpoint region in 3q21 is gene rich. Gene **193:**49–57.
63. **Saitoh, M., H. Nishitoh, M. Fujii, K. Takeda, K. Tobiume, Y. Sawada, M. Kawabata, K. Miyazono, and H. Ichijo.** 1998. Mammalian thioredoxin is a direct inhibitor of apoptosis signal-regulating kinase (ASK) 1. EMBO J. **17:**2596–2606.
64. **Seigneur, M., V. Bidnenko, S. D. Ehrlich, and B. Michel.** 1998. RuvAB acts at arrested replication forks. Cell **95:**419–430.
65. **Shen, X., G. Mizuguchi, A. Hamiche, and C. Wu.** 2000. A chromatin remodelling complex involved in transcription and DNA processing. Nature **406:** 541–544.
66. **Sommer, A., K. Bousset, E. Kremmer, M. Austen, and B. Luscher.** 1998. Identification and characterization of specific DNA-binding complexes containing members of the Myc/Max/Mad network of transcriptional regulators. J. Biol. Chem. **273:**6632–6642.
67. **Takeda, J., T. Maekawa, T. Sudo, Y. Seino, H. Imura, N. Saito, C. Tanaka, and S. Ishii.** 1991. Expression of the CRE-BP1 transcriptional regulator binding to the cyclic AMP response element in central nervous system, regenerating liver, and human tumors. Oncogene **6:**1009–1014.
68. **Tsai, E. Y., J. Jain, P. A. Pesavento, A. Rao, and A. E. Goldfeld.** 1996. Tumor necrosis factor alpha gene regulation in activated T cells involves ATF-2/Jun and NFATp. Mol. Cell. Biol. **16:**459–467.
69. **van Dam, H., M. Duyndam, R. Rottier, A. Bosch, L. de Vries-Smits, P. Herrlich, A. Zantema, P. Angel, and, A. J. van der Eb.** 1993. Heterodimer formation of cJun and ATF-2 is responsible for induction of c-jun by the 243 amino acid adenovirus E1A protein. EMBO J. **12:**479–487.
70. **van Dam, H., S. Huguier, K. Kooistra, J. Baguet, E. Vial, A. J. van der EB, P. Herrlich, P. Angel, and M. Castellazzi.** 1998. Autocrine growth and anchorage independence: two complementing Jun-controlled genetic programs of cellular transformation. Genes Dev. **12:**1227–1239.
71. **van Dam, H., D. Wilhelm, I. Herr, A. Steffen, P. Herrlich, and P. Angel.** 1995. ATF-2 is preferentially activated by stress-activated protein kinases to mediate c-jun induction in response to genotoxic agents. EMBO J. **14:**1798–1811.
72. **Wisdom, R., R. S. Johnson, and C. Moore.** 1999. c-Jun regulates cell cycle progression and apoptosis by distinct mechanisms. EMBO J. **18:**188–197.
73. **Wood, M. A., S. B. McMahon, and M. D. Cole.** 2000. An ATPase/helicase complex is an essential cofactor for oncogenic transformation by c-Myc. Mol. Cell **5:**321–330.
74. **Workman, J. L., and R. E. Kingston.** 1998. Alteration of nucleosome structure as a mechanism of transcriptional regulation. Annu. Rev. Biochem. **67:**545–579.